Optimization of Surface Flux Transport Models for the Solar Polar Magnetic Field

SOLARNET Summer school : A week above the sky

5-9 Aug, 2019 Tenerife, Spain

Mohammed H. Talafha & Kristof Petrovay
Dept. of Astronomy, Eötvös Loránd University
Budapest, Hungary

Surface Flux Transportation Model (SFT)

- The magnetic flux is dispersed and transported with the plasma by surface flows, and locally destroyed or amplified according to basic rules of electromagnetic induction, this process is well described by the MHD induction equation

$$\frac{\partial B}{\partial t} = \nabla \times (u \times B - \eta \nabla \times B)$$

- considering the magnetic field to be predominantly radial on global scales solving only the r-component of previous equation, after enforcing the null divergence condition throughout:

$$\frac{\partial B_R}{\partial t} = -\frac{1}{R \sin\theta}\frac{\partial}{\partial\theta}[u_\theta(R,\theta) B_R \sin\theta] - \Omega(R,\theta)\frac{\partial B_R}{\partial\varphi} + \frac{\eta_R}{R^2}\left[\frac{1}{\sin\theta}\frac{\partial}{\partial\theta}\left(\sin\theta\frac{\partial B}{\partial\theta}\right) + \frac{1}{sin^2\theta}\frac{\partial^2 B_R}{\partial\phi^2}\right] - \frac{B_R}{\tau_R} + S_{BMR}(\theta,\phi,t)$$

Constraints

- The WSO polar field gives the line of sight components of the magnetic field averaged over the pole most aperture of the instrument, roughly at latitudes above 55 degrees.

$$\breve{B}_l = \frac{1}{\tilde{\tilde{N}}} \int_0^{\theta_0} B_R \sin^2\theta \; d\theta$$

- Around activity minima, the axial dipole moment is dominated by the polar fields and represents the relevant quantity for the poloidal magnetic flux connected to the polar fields.

$$D^*(t) = \frac{2}{3} \int_0^{\pi} < B_R >^{\varphi} (\theta, t) \cos\theta \sin\theta \, d\theta$$

WSO: Wilcox Solar Observatory

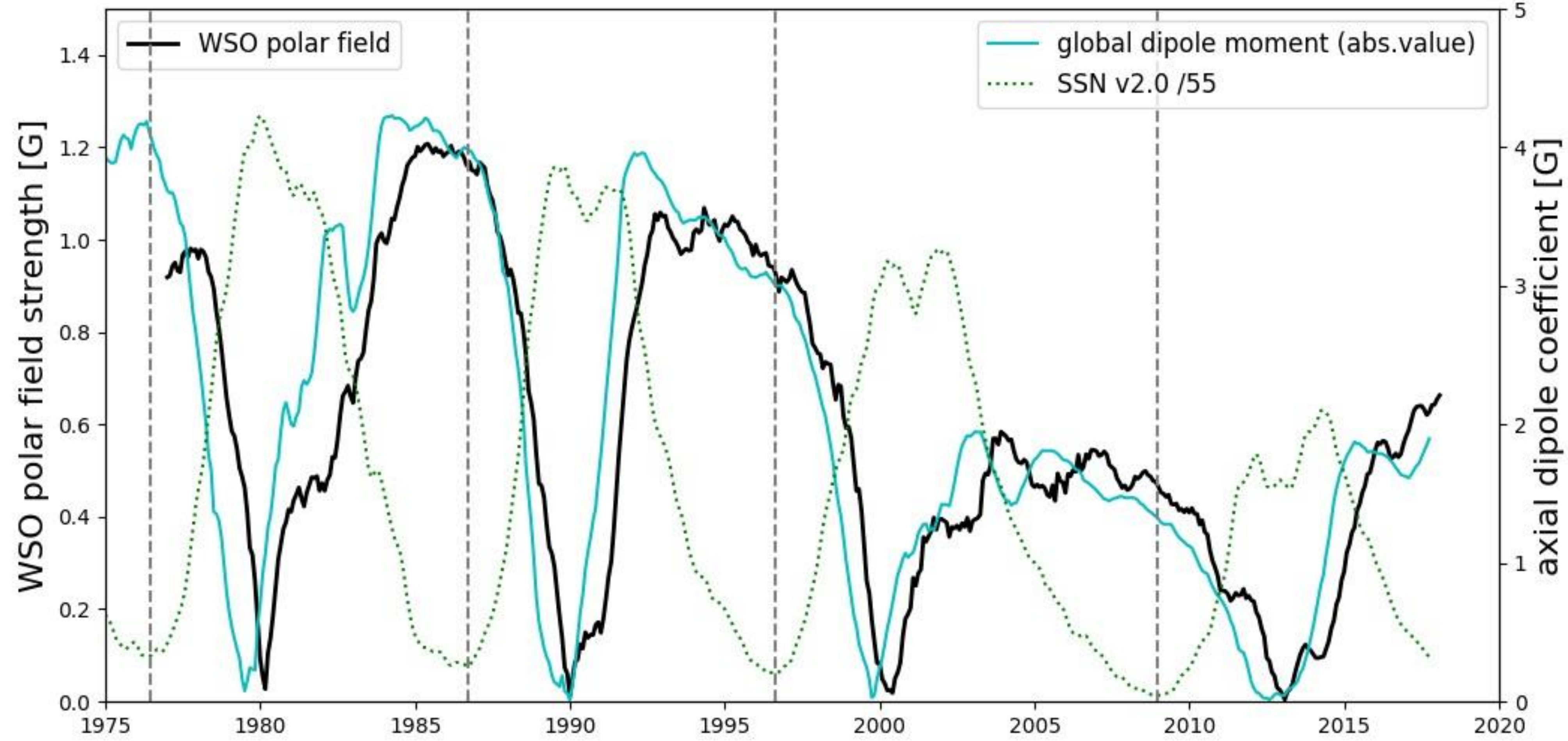

WSO polar field
global dipole moment (abs.value)
SSN v2.0 /55
WSO polar field strength [G]
axial dipole coefficient [G]
1.4
1.2
1.0
0.8
0.6
0.4
0.2
0.0
5
4
3
2
1
0
1975
1980
1985
1990
1995
2000
2005
2010
2015
2020

Parameter	**Mean**	**Std(σ)**
revWSOB	4.33	0.36
revdipmom	3.44	0.18
relWSOB	0.94	0.07
reldipomom	0.8	0.11
hmcycmin	70	2.5

Computations

- Python script include
  - **Source function:** represented by a pair of rings of opposite magnetic polarity.
  - **Meridional flow profiles :**
    - (Dikpati et al. 2006) and (Cameron & Schüssler 2007). $u_c = u_o \sin(\pi \times \lambda/90)$
    - (Van Ballegooijen et al. 1998); used by (Jiang et al. 2014). $$u_c = \begin{cases} u_0 \sin\left(\pi \times \dfrac{\lambda}{90}\right) & \text{if } |\lambda| < {}_o\lambda \\ 0 & otherwise \end{cases}$$
    - (Lemerle & Charbonneau 2017). $u_c(R,\theta) = -\dfrac{u_0}{u_0{}^*}\, erf^q(v \sin\theta) erf^n(w \cos\theta)$
  - **Diffusivity:** values (η) (50 - 750) $km^2 s^{-1}$.
  - **Source decay time:** values (τ) (2 - 100) yr.
  - **Meridional flow velocity:** values (u_o) (5 – 20) ms^{-1}.

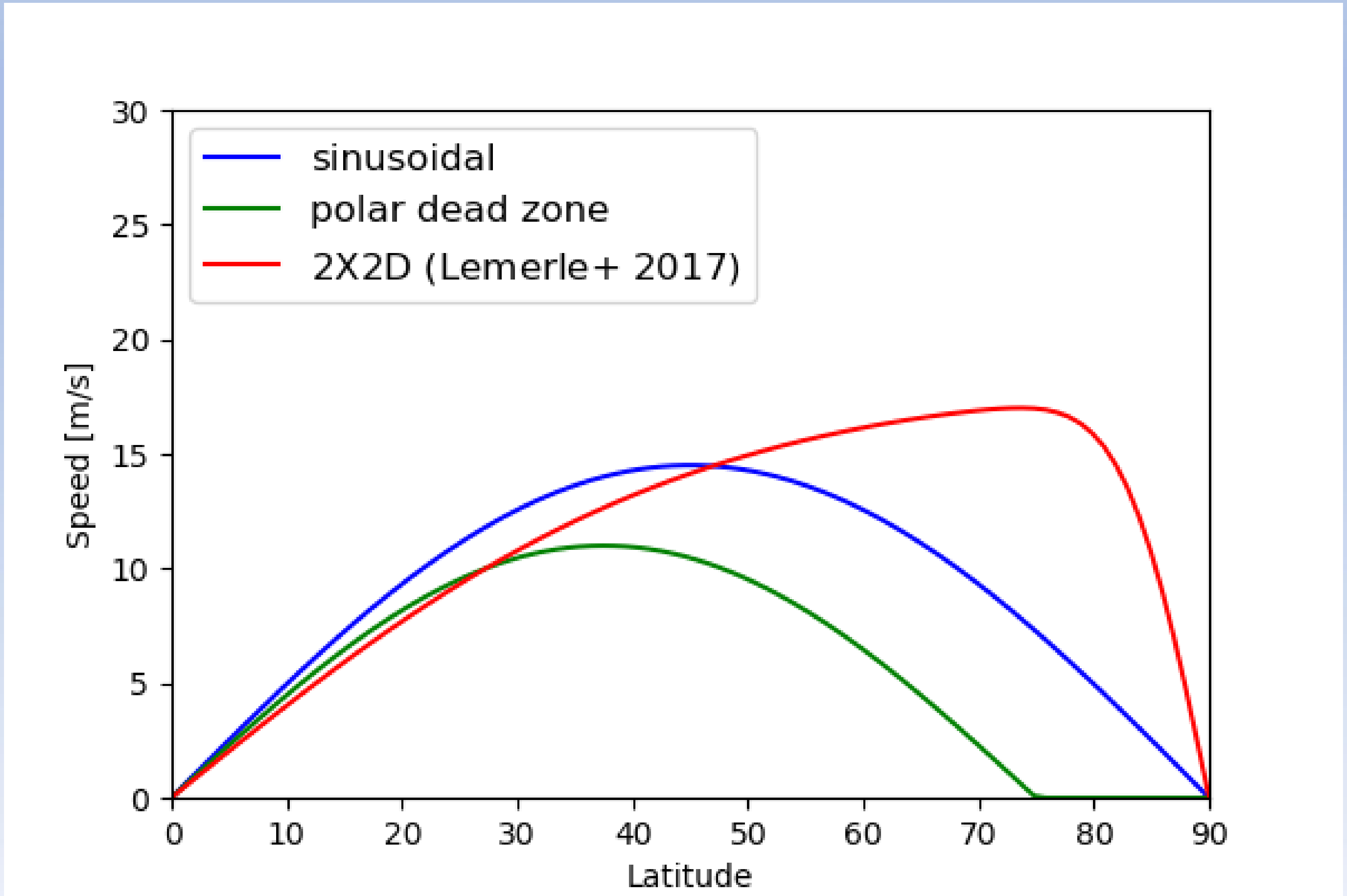
sinusoidal
polar dead zone
2X2D (Lemerle+ 2017)
Speed [m/s]
Latitude
0
5
10
15
20
25
30
0
10
20
30
40
50
60
70
80
90

The code was run for 50 Solar cycle, where the results taken for the last two cycles.

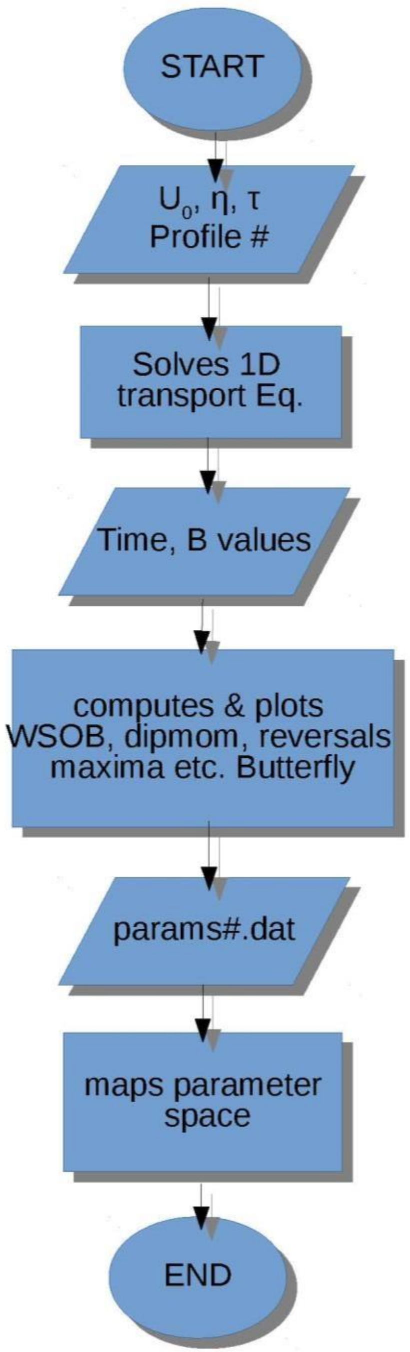

Results

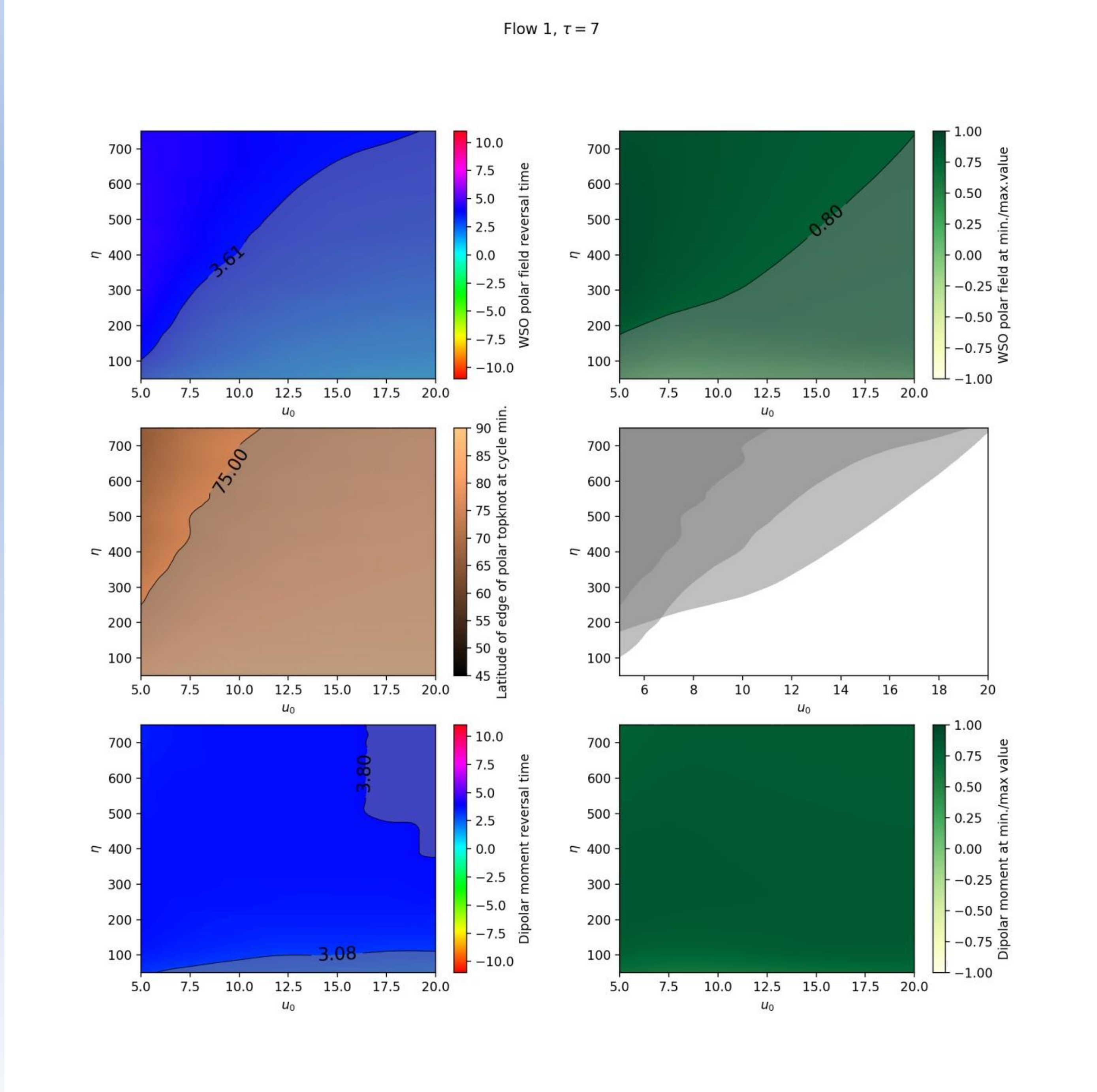

Flow 1, $\tau = 7$
WSO polar field reversal time
WSO polar field at min./max.value
Latitude of edge of polar topknot at cycle min.
Dipolar moment reversal time
Dipolar moment at min./max value
3.61
0.80
75.00
3.80
3.08
η
u_0

Good solution

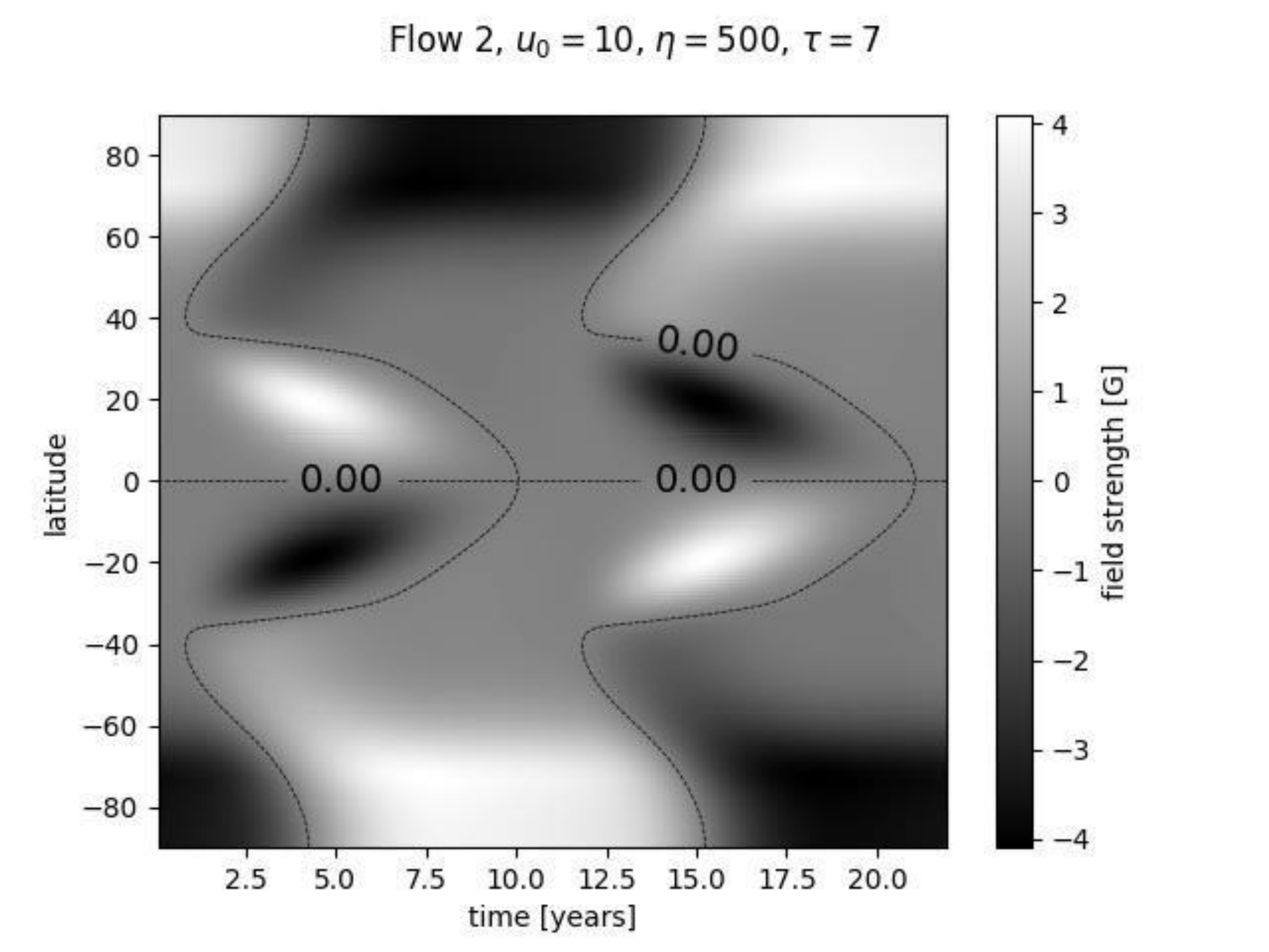

Example of a solution satisfying all observational constraints on the polar magnetic field: temporal variation and latitudinal profiles.

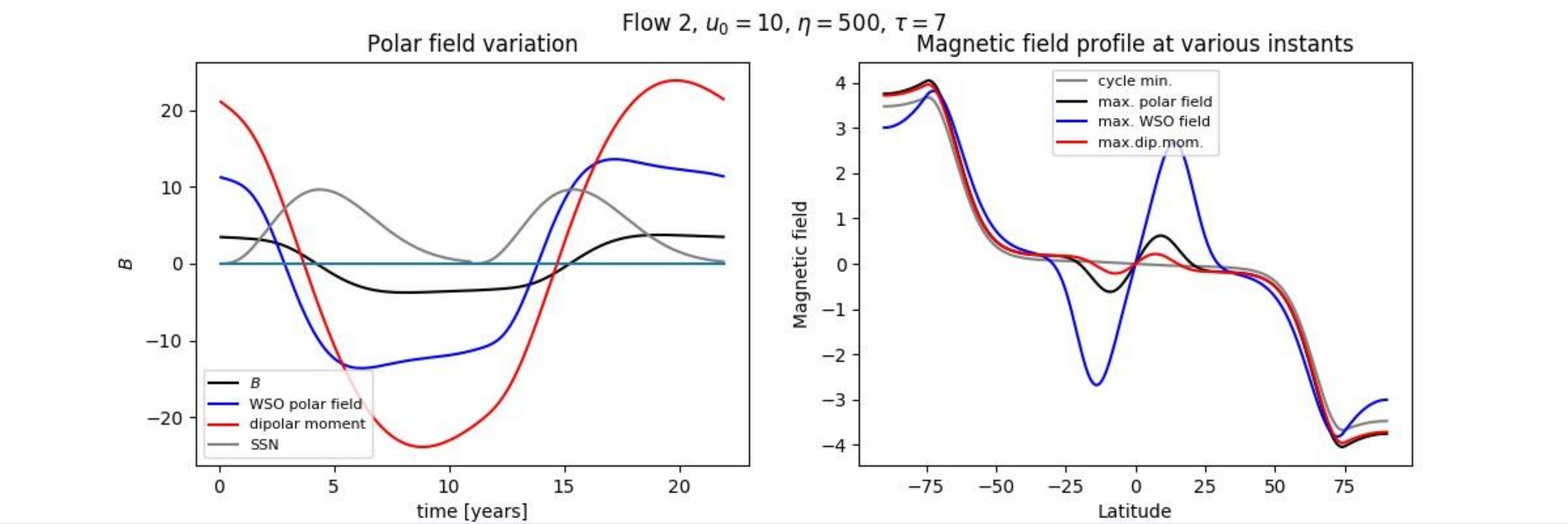

Results

- The parabolic latitudinal profile (Jiang et al. 2011) in the source function is more realistic one than the linear one (Cameron et al. 2007) which was to measure how robustly and sensitivity was the choice.
- The rate of creation of dipole moment is mostly determined by the divergence of the meridional flow near the equator.
- The time variation of the dipole moment primarily depends on τ.
- The range of τ lies somewhere between 5 and 10 years for all three flow types considered.
- Solutions with higher diffusivity values (500 $\frac{Km^2}{s}$ and above) tend to be favored, Some models with lower diffusivity are still allowed.

- For the 2nd meridional flow profile (a flow with a polar dead zone), the allowed range is most extensive for τ=7, mostly characterized by higher values of η and also of u_0 (15m/s, for τ = 10 it produces too late dipole reversals.
- The pole-reaching flows (type 1 and 3), the allowed domain that exists in the range τ ~ 5 to 9 invariably lies in the top left part of our parameters plane, i.e. combinations with higher diffusivity and lower flow speed are preferred.
- With the flow profile obtained in the 2×2D dynamo model of Lemerle & Charbonneau (2017) polar fields will only show fully solar-like behaviour for $\eta/u_0 \gtrsim 150$ (e.g. for $u_0 \gtrsim 5$ m/s, $\eta \gtrsim 700$ km^2/s) and τ ~ 5–9 yr.

Thank you

Source Function

$$S(\lambda,t) = kA_m S_1(t) S_2(\lambda; \lambda_o(t) - \Delta\lambda(t), \delta\lambda)$$
$$- kA_m S_1(t) S_2(\lambda; \lambda_o(t) + \Delta\lambda(t), \delta\lambda)$$
$$+ kA_m S_1(t) S_2(\lambda; -\lambda_o(t) - \Delta\lambda(t), \delta\lambda)$$
$$- kA_m S_1(t) S_2(\lambda; -\lambda_o(t) + \Delta\lambda(t), \delta\lambda)$$

$$2\Delta\lambda = 0.5 \frac{\sin\lambda}{\sin 20^o}$$

$$\lambda_o[o] = 26.4 - \frac{34.2t}{P} + 16.1\left(\frac{t}{P}\right)^2$$

$$S_1(t) = at_c^3/[\exp\left(\frac{t_c^2}{b^2}\right) - c]$$

- k : is a factor alternating between even and odd cycles.
- A_m : is an arbitrary amplitude depending on the flow profile (0.003, 0.015 and 0.0005 for our three profiles.
- $S_2(\lambda; \lambda_o(t), \delta\lambda)$ is the latitudinal profile represented by a Gaussian with a fixed FWHM of $2\delta\lambda = 6^o$, migrating equatorward during the course of a cycle.
- The latitudinal separation of the rings is a consequence of Joy's law.
- their trajectory during the course of a cycle is given by a quadratic fit from Jiang et al. 2011.
- the time profile of solar activity in a typical cycle was determined by Hathaway et al. 1994, from the average of many cycles

References

- Cameron, R., Sch•ussler, M.: The Astrophysical Journal 659(1), 801 (2007)
- Charbonneau, P.: Annual Review of Astronomy and Astrophysics 52, 251 (2014)
- Dikpati, M., De Toma, G., Gilman, P.A.: Geophysical research letters 33(5) (2006)
- Hathaway, D.H., Wilson, R.M., Reichmann, E.J.: Solar Physics 151(1), 177 (1994)
- Jiang, J., Isik, E., Cameron, R., Schmitt, D., Sch•ussler, M.: The Astrophysical Journal 717(1), 597 (2010)
- Jiang, J., Hathaway, D., Cameron, R., Solanki, S., Gizon, L., Upton, L.: Space Science Reviews 186(1-4), 491 (2014)
- Jiang, J., Wang, J.-X., Jiao, Q.-R., Cao, J.-B.: The Astrophysical Journal 863(2), 159 (2018)
- Lemerle, A., Charbonneau, P.: The Astrophysical Journal 834(2), 133 (2017)
- Lemerle, A., Charbonneau, P., Carignan-Dugas, A.: The Astrophysical Journal 810(1), 78 (2015)
- S. Wedemeyer-Böhm, A. Lagg, Å. Nordlund, Space Sci Rev. 144 : 317-350, (2009)
- SILSO: 2018 The International Sunspot Number. http://www.sidc.be/silso/Stanford, U.: 2006 Wilcox Solar Observatory Polar Field Observations. http://wso.stanford.edu/Polar.html
- Van Ballegooijen, A.Cartledge, N., Priest, E.: The Astrophysical Journal 501(2), 866 (1998)